

Perfusion chromatography: performance of periodic countercurrent column operation and its comparison with fixed-bed operation

G.A. Heeter, A.I. Liapis*

Department of Chemical Engineering and Biochemical Processing Institute, University of Missouri-Rolla, Rolla, MO 65401-0249, USA

Abstract

Simulation studies using mathematical models that describe the single-component adsorption of bovine serum albumin into spherical bidisperse perfusive and spherical bidisperse purely diffusive anion-exchange porous adsorbent particles in a single-column fixed-bed system and in a two-column periodic countercurrent system in which the adsorbent is equally distributed over two beds are presented. The total length of the two-column periodic countercurrent system is equal to the length of the single-column fixed-bed system, and studies are performed for different values of the intraparticle Peclet number, Pe_{intra} , and of the microsphere diameter, d_m . In the single-column fixed-bed system, the percentage utilization of the adsorptive capacity of the adsorbent increases as d_m decreases and Pe_{intra} increases. The results indicate that the two-column system under periodic countercurrent operation provides higher values for the percentage utilization of the adsorptive capacity of the adsorbent than all the values of the percentage utilization of the adsorptive capacity of the adsorbent obtained from the single-column fixed-bed system for all values of d_m and Pe_{intra} examined in this work. It is an interesting result that the percentage utilization of the adsorptive capacity obtained from a two-column periodic counter-current system having purely diffusive ($Pe_{intra} = 0$) adsorbent particles with the largest microsphere size, d_m , studied in this work is found to be higher than the percentage utilization of the adsorptive capacity obtained from a single-column system that uses perfusive adsorbent particles with the smallest microsphere size, d_m , and the largest intraparticle Peclet number, Pe_{intra} , studied in this work. The simulation studies with the two-column periodic countercurrent system also provide the following interesting result: the factors of economic significance in the two-column system under periodic countercurrent operation, namely the time between column switches and the degree of saturation of the column removed, are nearly independent of the values of the microsphere diameter, d_m , and the intraparticle Peclet number, Pe_{intra} .

1. Introduction

In this work, as in previous publications [1–6], we define “perfusion chromatography” to refer to any chromatographic system in which the

intraparticle convective velocity, v_p , is non-zero [1–8].

Liapis and McCoy [4] and Liapis et al. [5] have considered that the perfusive adsorbent particles with a bidisperse [4,5] porous structure have a macroporous region, made by the through-pores [1,3–5,7] in which intraparticle convection and pore diffusion occur, and a microporous [4,5]

* Corresponding author.

region, made by spherical microparticles (micro-spheres [4,5,7]) that are taken to be purely diffusive. In this work, the mathematical model constructed by Liapis et al. [5], which could describe adsorption in columns having spherical porous structure, is solved and used to study the behavior of periodic countercurrent and fixed-bed systems involving the adsorption of bovine serum albumin (BSA) into spherical anion-exchange porous particles. The performance of chromatographic columns, as measured by the percentage utilization of the capacity of the adsorbent in the column and the time between bed switches for periodic countercurrent systems or the period of the operating cycle for single-column fixed bed systems, is compared for both single-column fixed-bed and two-column periodic countercurrent systems for different values of the microsphere diameter, d_m , and the intraparticle Peclet number, Pe_{intra} . The total length of the two-column periodic countercurrent system is equal to the length of the single-column fixed-bed system.

2. Periodic countercurrent operation

The employment of affinity adsorption chromatography as an efficient and competitive separation process, when compared to other separation methods, requires the effective use of the active sites of the adsorbent particles. It has been shown [9,10] that the utilization of the active sites of purely diffusive adsorbent particles could be substantially increased if periodic countercurrent operation is employed in the adsorption process. The most efficient mode of operation would theoretically be the continuous [9] countercurrent operation where the adsorbent particles move in a direction opposite to the direction of motion of the flowing fluid stream; however, this mode of operation would have practical problems because of mechanical complexity of the equipment, gradual attrition of the solid adsorbent, and channeling (non-uniform flow) of either fluid or solid. Therefore, it could be easier to use a periodic countercurrent mode

of operation since, if a column is divided into an infinite number of infinitesimal-in-size beds operating in a periodic countercurrent mode, this would give the same results as the continuous countercurrent mode of operation.

In practice one has to deal with finite bed sizes and, therefore, the original column is subdivided into a number of smaller-in-size columns that operate in a periodic countercurrent mode. In Fig. 1 a column of length L has been divided into two columns, each of length $L/2$, that operate in a periodic countercurrent mode during the adsorption stage. Three columns, each of length $L/2$, are shown in the system of Fig. 1 since one column of length $L/2$ is always under regeneration. In a periodic countercurrent operation a column switch occurs, as in the case of fixed-bed operation, when the outlet concentration of the adsorbate reaches a certain percentage of its inlet value.

In this work, the performance of the adsorption of BSA into spherical anion-exchange bidisperse porous particles packed in a column operating under the periodic countercurrent mode of operation is studied for different values of the intraparticle Peclet [5] number, Pe_{intra} , and of the microsphere [5] diameter, d_m . The results are compared with those obtained when the column is operating under the fixed-bed

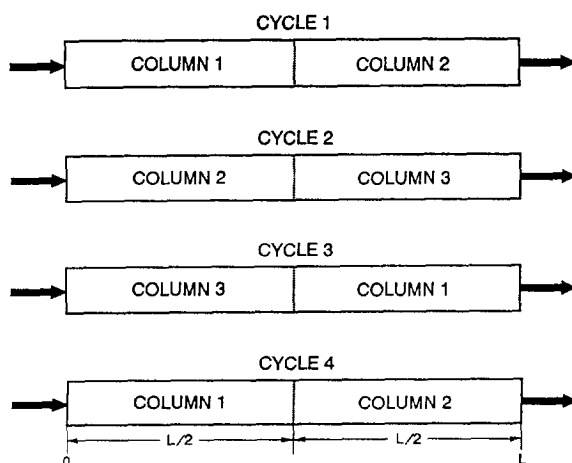


Fig. 1. Principal arrangement of two columns, each of length $L/2$, in a periodic countercurrent operation where L is the total operating length. The system employs three columns, but one is always under regeneration.

mode of operation. It is appropriate to mention at this point that the adsorbent particles are considered to be purely diffusive when the intraparticle Peclet number is equal to zero, while the adsorbent particles are considered to be perfusive when the intraparticle Peclet number is greater than zero.

3. Mathematical model for fixed bed

Adsorption is considered to take place from a flowing liquid stream in a fixed bed of spherical perfusive adsorbent particles of bidisperse porous structure under isothermal conditions. The differential mass balance for the adsorbate in the flowing fluid stream gives [1,2,4–6]

$$\frac{\partial C_d}{\partial t} - D_L \frac{\partial^2 C_d}{\partial x^2} + \frac{V_t}{\varepsilon} \frac{\partial C_d}{\partial x} = - \frac{(1 - \varepsilon)}{\varepsilon} \frac{\partial \bar{C}_{ps}}{\partial t} \quad (1)$$

The initial and boundary conditions of Eq. 1 are as follows:

$$\text{at } t = 0, C_d = 0, 0 \leq x \leq L \quad (2)$$

$$\text{at } x = 0, \frac{V_t}{\varepsilon} C_d \Big|_{x=0} - D_L \frac{\partial C_d}{\partial x} \Big|_{x=0} = \frac{V_t}{\varepsilon} C_{d,in}, \quad t > 0 \quad (3)$$

$$\text{at } x = L, \frac{\partial C_d}{\partial x} \Big|_{x=L} = 0, t > 0 \quad (4)$$

The value of $C_{d,in}$ may be constant or it may vary with time. An expression for estimating D_L was presented by Arnold et al. [11], but in certain systems the axial dispersion is so low that by setting its value equal to zero the error introduced in the prediction of the behavior of an affinity adsorption system is not significant [11,12]. When the axial dispersion coefficient is set equal to zero, Eq. 3 (with $D_L = 0$) becomes as follows:

$$\text{at } x = 0, C_d = C_{d,in}, t > 0 \quad (5)$$

The spherical perfusive adsorbent particles with a bidisperse [4,5] porous structure are considered to have a microporous [4,5] region made by spherical microparticles (microspheres [4,5,7]) that are taken to be purely diffusive, and

SPHERICAL BIDISPERSE PERFUSIVE PARTICLE

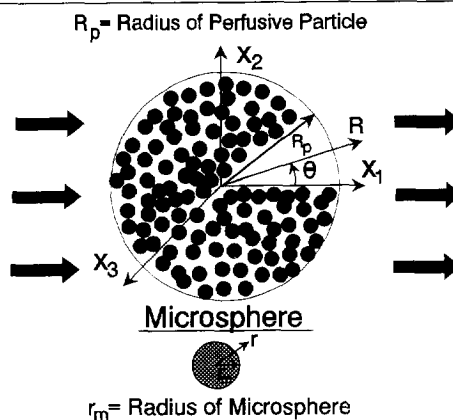


Fig. 2. Spherical perfusive adsorbent particle with a bidisperse porous structure (the arrows indicate the direction of fluid flow).

a macroporous [4,5] region made by the throughpores [1,3–5,7] in which intraparticle convection and pore diffusion occur. In Fig. 2, a diagram of a spherical perfusive adsorbent particle with a bidisperse porous structure is shown; x_1 represents the axial coordinate for the spherical perfusive adsorbent particle and is parallel to the axial coordinate x of the column.

The differential mass balance for the adsorbate in the macroporous region of a perfusive adsorbent particle of spherical geometry is given by

$$\begin{aligned} \varepsilon_p \frac{\partial C_p}{\partial t} + \varepsilon_p v_{pR} \frac{\partial C_p}{\partial R} + \varepsilon_p v_{p\theta} \left(\frac{1}{R} \right) \frac{\partial C_p}{\partial \theta} \\ + (1 - \varepsilon_p) \frac{\partial \bar{C}_s}{\partial t} = \varepsilon_p D_p \left[\left(\frac{1}{R^2} \right) \frac{\partial}{\partial R} \left(R^2 \frac{\partial C_p}{\partial R} \right) \right. \\ \left. + \left(\frac{1}{R^2 \sin \theta} \right) \frac{\partial}{\partial \theta} \left(\sin \theta \frac{\partial C_p}{\partial \theta} \right) \right] \quad (6) \end{aligned}$$

The variables v_{pR} and $v_{p\theta}$ represent the intraparticle velocity components along the R and θ directions, respectively. Neale et al. [13] have obtained analytical expressions for the stream functions outside and inside the permeable spheres. By using the expression of Neale et al. [13] for the stream function inside the particle, the following equations for v_{pR} and $v_{p\theta}$ are obtained:

$$v_{pR} = V_f \cos \theta \left[F - \left(\frac{H}{\xi^2} \right) \left(\frac{\sinh \xi}{\xi} - \cosh \xi \right) \right] \quad (7)$$

$$v_{p\theta} = -V_f \sin \theta \left[F - \left(\frac{H}{2\xi} \right) \left(\frac{\xi \cosh \xi - \sinh \xi}{\xi^2} - \sinh \xi \right) \right] \quad (8)$$

The expressions for ξ , F , and H are presented in Refs. [5] and [13] and will not be reported again here. The axial component of the intraparticle velocity, v_{px_1} , which is parallel to the flowing fluid stream along the axis of the column, is given by

$$v_{px_1} = v_{pR} \cos \theta - v_{p\theta} \sin \theta \quad (9)$$

Liapis et al. [5] have indicated that the value of v_{px_1} becomes independent of the values of R and θ when $H = 0$ in Eqs. 7 and 8. It has been found [5,14] from numerous parametric calculations that for various adsorption systems the value of H in Eqs. 7 and 8 is essentially equal to zero. When H is taken to be approximately equal to zero ($H \cong 0$) in Eqs. 7 and 8, the following expressions for v_{pR} , $v_{p\theta}$, and v_{px_1} are obtained:

$$v_{pR} \cong FV_f \cos \theta \quad (10)$$

$$v_{p\theta} \cong -FV_f \sin \theta \quad (11)$$

$$v_{px_1} = FV_f \quad (12)$$

If the intraparticle Peclet number, Pe_{intra} , is defined by Eq. 13

$$Pe_{intra} = \frac{v_{px_1} d_p}{D_p} \quad (13)$$

then by using the expression for v_{px_1} given in Eq. 12 the following expression for Pe_{intra} is obtained:

$$Pe_{intra} = \frac{v_{px_1} d_p}{D_p} = \frac{(FV_f) d_p}{D_p} \quad (14)$$

For purely diffusive adsorbent particles $Pe_{intra} = 0$, while for adsorbent particles with non-zero intraparticle fluid flow $Pe_{intra} > 0$. The value of H for the adsorption system considered in this work is approximately equal to zero, and therefore,

the values of v_{pR} , $v_{p\theta}$, v_{px_1} , and Pe_{intra} are obtained from Eqs. 10, 11, 12, and 14, respectively.

The initial and boundary conditions of Eq. 6 are as follows:

$$\text{at } t = 0, C_p = 0, 0 \leq R \leq R_p \quad (15)$$

$$\text{at } R = R_p, C_p = C_d, t > 0, 0 \leq \theta \leq \pi \quad (16)$$

$$\text{at } R = 0, C_p = \text{finite}, t > 0, 0 \leq \theta \leq \pi \quad (17)$$

$$\text{at } \theta = 0, \left. \frac{\partial C_p}{\partial \theta} \right|_{\theta=0} = 0, 0 \leq R \leq R_p \quad (18)$$

$$\text{at } \theta = \pi, \left. \frac{\partial C_p}{\partial \theta} \right|_{\theta=\pi} = 0, 0 \leq R \leq R_p \quad (19)$$

The differential mass balance for the adsorbate in a purely diffusive spherical microparticle (microsphere) is given by [4,5]

$$\begin{aligned} \varepsilon_{pm} \frac{\partial C_{pm}}{\partial t} + \left(\frac{1}{1 - \varepsilon_p} \right) \frac{\partial C_{sm}}{\partial t} \\ = \varepsilon_{pm} D_{pm} \left(\frac{\partial^2 C_{pm}}{\partial r^2} + \frac{2}{r} \frac{\partial C_{pm}}{\partial r} \right) \end{aligned} \quad (20)$$

The accumulation term, $\partial C_{sm} / \partial t$, of the adsorbed species can be quantified if a thermodynamically consistent mathematical model could be constructed that could describe the mechanism of adsorption for the adsorbate. For isothermal adsorption systems, the term $\partial C_{sm} / \partial t$ could be of the form

$$\frac{\partial C_{sm}}{\partial t} = f(C_{pm}, C_{sm}, \mathbf{k}) \quad (21)$$

where f represents the functional form of the dynamic adsorption mechanism for the adsorbate, and \mathbf{k} represents the vector of the rate constants that characterize the interaction kinetics between the adsorbate molecules and the active sites. One well known form of Eq. 21 for single-component adsorption ($A + S \xrightleftharpoons[k_2]{k_1} AS$) is as follows [1,4–6]:

$$\frac{\partial C_{sm}}{\partial t} = k_1 C_{pm} (C_T - C_{sm}) - k_2 C_{sm} \quad (22)$$

The term $\partial C_{sm} / \partial t$ in Eq. 20 could now be replaced by the right-hand-side of Eq. 22. The

initial and boundary conditions of Eqs. 20 and 21 (as well as of Eq. 22) are considered to be as follows:

$$\text{at } t = 0, C_{pm} = 0, 0 \leq r \leq r_m \quad (23)$$

$$\text{at } t = 0, C_{sm} = 0, 0 \leq r \leq r_m \quad (24)$$

$$\text{at } r = r_m, C_{pm} = C_p(t, R, \theta), t > 0 \quad (25)$$

$$\text{at } r = 0, \left. \frac{\partial C_{pm}}{\partial r} \right|_{r=0} = 0, t > 0 \quad (26)$$

The accumulation term $\partial \bar{C}_s / \partial t$ in Eq. 6 is given [5] by Eq. 27

$$\begin{aligned} \frac{\partial \bar{C}_s}{\partial t} = & \frac{3}{r_m^3} \left[\frac{\partial}{\partial t} \left(\int_0^{r_m} \varepsilon_{pm} C_{pm} r^2 dr \right) \right. \\ & \left. + \frac{\partial}{\partial t} \left(\int_0^{r_m} \left(\frac{1}{1 - \varepsilon_p} \right) C_{sm} r^2 dr \right) \right] \quad (27) \end{aligned}$$

The term $\partial \bar{C}_{ps} / \partial t$ in Eq. 1 is obtained [5] from Eq. 28:

$$\begin{aligned} \frac{\partial \bar{C}_{ps}}{\partial t} = & \frac{3}{2R_p^3} \left[\frac{\partial}{\partial t} \left(\int_0^\pi \int_0^{R_p} \varepsilon_p C_p R^2 \sin \theta dR d\theta \right) \right. \\ & \left. + \frac{\partial}{\partial t} \left(\int_0^\pi \int_0^{R_p} (1 - \varepsilon_p) \bar{C}_s R^2 \sin \theta dR d\theta \right) \right] \quad (28) \end{aligned}$$

Finally, for a given pair of values of R and θ the average concentration of the adsorbate in the adsorbed phase, \bar{C}_{sa} , is obtained [5] from the following expression:

$$\bar{C}_{sa} = (1 - \varepsilon_p) \frac{3}{r_m^3} \left[\int_0^{r_m} \left(\frac{1}{1 - \varepsilon_p} \right) C_{sm} r^2 dr \right] \quad (29)$$

The dynamic behavior of a column adsorption system involving spherical perfusive adsorbent particles with a bidisperse porous structure could be obtained by solving simultaneously Eqs. 1, 6, 20, and 21. It should be noted that Eq. 22 could be used for Eq. 21 with the understanding that Eq. 22 represents only one possible form of Eq. 21. If the intraparticle velocity is zero ($v_{pR} =$

$v_{p\theta} = 0$), then the spherical adsorbent particles are considered to be purely diffusive. In this case, the concentration C_p is considered to be independent of θ and, thus, the term $\partial C_p / \partial \theta$ in Eq. 6 is taken to be equal to zero; furthermore, the boundary conditions given by Eqs. 18 and 19 are not needed, and the boundary condition at $R = 0$ becomes $(\partial C_p / \partial R)|_{R=0} = 0$.

The solution of Eqs. 1, 6, 20, and 22 was obtained by using the numerical solution procedure reported in Ref. [5].

4. Mathematical model for periodic countercurrent operation

The mathematical model that describes periodic countercurrent adsorption is the same as that of a fixed bed. The solution procedure for the single-column case can easily be adapted to the multicolumn problem. After a column has been removed from the end of the sequence of columns corresponding to the fluid input and replaced by a fresh column at the other end, the initial conditions must be adjusted for the start of the new operating period. That part of the profile is deleted which corresponds to the column that has been removed. The profile of the remaining columns is shifted, and the profile of the newly regenerated column is added at the other end.

The criterion for when to remove the bed at the upstream fluid end and to introduce a fresh bed at the other end can be based on the outlet concentration of the adsorbate.

5. Results and discussion

In this work, the efficiency with which anion-exchange porous adsorbent particles are utilized by the adsorption of BSA is compared for a single fixed-bed and a periodic countercurrent system in which the adsorbent is equally distributed over two beds (as shown in Fig. 1). The comparison is made for different values of the intraparticle Peclet number, Pe_{intra} , and of the microparticle (microsphere) diameter, d_m . The

diameter of the adsorbent particles, d_p , is taken to be $1.5 \cdot 10^{-5}$ m, while three different values for the diameter of the microparticles, d_m , were employed in the studies of this work: (a) $d_m = 7.0 \cdot 10^{-8}$ m; (b) $d_m = 7.0 \cdot 10^{-7}$ m; and (c) $d_m = 7.0 \cdot 10^{-6}$ m. The value of H (Eqs. 7 and 8) for the adsorption system considered in this work is approximately equal to zero and, therefore, the values of v_{pR} , $v_{p\theta}$, v_{px_1} , and Pe_{intra} are obtained from Eqs. 10, 11, 12 and 14, respectively. For purely diffusive adsorbent particles $Pe_{intra} = 0$, while for adsorbent particles with non-zero intraparticle fluid flow $Pe_{intra} > 0$. In this work, the Pe_{intra} given by Eq. 14 was varied between 0 and 100 ($0 \leq Pe_{intra} \leq 100$); in the simulation studies of this work the values of d_p , V_f , and D_p were kept constant and, therefore, the value of Pe_{intra} was varied between 0 and 100 by appropriately changing the value of F in Eq. 14. In Table 1, the values of the parameters used for the simulations of the adsorption system studied in this work are presented. The value of C_s^* in Table 1 is obtained from the following expression:

$$C_s^* = \frac{C_T K C_{d,in}}{1 + K C_{d,in}} \quad (30)$$

The value of C_s^* represents the equilibrium value of the concentration of the adsorbate in the adsorbed phase when the equilibrium value of the concentration of the adsorbate in the fluid phase is equal to $C_{d,in}$. Furthermore, the value of $C_{d,in} = 0.1$ kg/m³ in Table 1 indicates that the value of the inlet concentration of the adsorbate in the flowing fluid stream remains constant for all times of the adsorption stage, and this indicates that the simulation studies of this work examine systems of frontal analysis.

In Fig. 3, the breakthrough curves of the single fixed bed are presented for two different microsphere sizes and three different intraparticle Peclet numbers. The breakthrough curves for the system with $d_m = 7.0 \cdot 10^{-8}$ m are not shown in Fig. 3; however, for the same values of Pe_{intra} the breakthrough curve obtained from the system having $d_m = 7.0 \cdot 10^{-8}$ m was found to be almost identical to the breakthrough curve obtained from the system having $d_m = 7.0 \cdot 10^{-7}$ m. The results in Fig. 3 indicate that as the microsphere size, d_m , decreases and the intraparticle Peclet number, Pe_{intra} , increases the breakthrough curve becomes steeper and the time at which breakthrough starts is increased. Thus, the utilization of the capacity of the adsorbent particles of the single fixed bed is increased as d_m is decreased and Pe_{intra} is increased; these results are in agreement with those obtained by Liapis et al. [5].

In Figs. 4a–7a, the dimensionless isoconcentration profiles of the adsorbate in the pore fluid of the pores of the macroporous region of the adsorbent particle are presented, while in Figs. 4b–7b the dimensionless isoconcentration profiles in the adsorbed phase of the adsorbent particles are shown, at position $x = 0.25L = 0.025$ m of the single fixed bed and at time $t = 36$ min. In Figs. 4–7 the outermost contours represent the isoconcentrations at the surface ($R = R_p$) of the particle, and the data in Figs. 4–7 have been obtained with $d_m = 7.0 \cdot 10^{-7}$ m. The effect of increasing Pe_{intra} is clearly shown through the change in the symmetry of the isoconcentration profiles of the adsorbate in the adsorbent particle. Examination of the concentration contours of Fig. 4 and Fig. 6, for $Pe_{intra} = 0$ and $Pe_{intra} = 10$, respectively, shows that there

Table 1

Values of the parameters of the column systems involving the adsorption of BSA into spherical bidisperse anion-exchange porous adsorbent particles

$$L = 0.1 \text{ m}, V_f = 2.778 \cdot 10^{-3} \text{ m}^3/\text{s}, d_p = 1.5 \cdot 10^{-5} \text{ m},$$

$$\varepsilon = 0.35, \varepsilon_p = 0.45, \varepsilon_{pm} = 0.50, T = 296 \text{ K},$$

$$D_L = 0, D_p = 13.27 \cdot 10^{-12} \text{ m}^2/\text{s}, D_{pm} = 7.08 \cdot 10^{-12} \text{ m}^2/\text{s},$$

$$C_{d,in} = 0.1 \text{ kg/m}^3, C_T = 78.3 \text{ kg/m}^3 \text{ particle}, C_s^* = 34.8 \text{ kg/m}^3 \text{ particle},$$

$$k_1 = 1.05 \text{ m}^3/\text{kg} \cdot \text{s}, k_2 = 0.131 \text{ s}^{-1}, K = 8.015 \text{ m}^3/\text{kg}$$

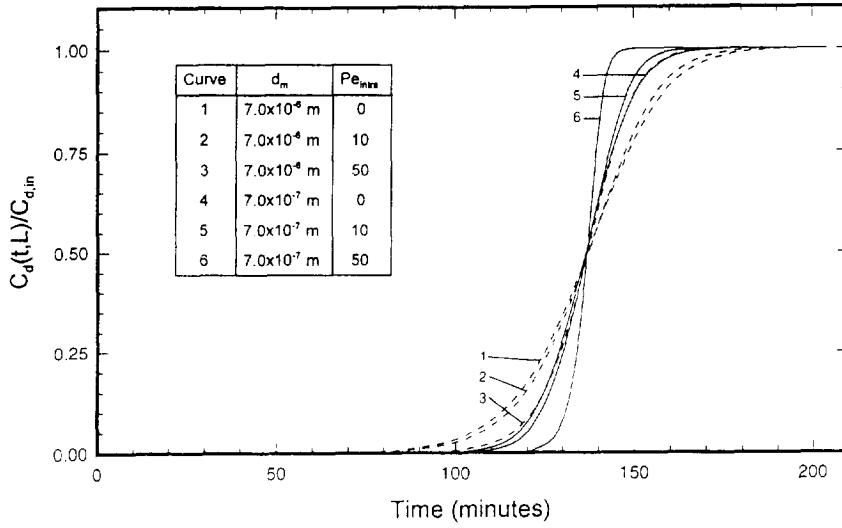


Fig. 3. Breakthrough curves obtained from the single-column fixed-bed system for different values of the microsphere diameter, d_m , and intraparticle Peclet number, Pe_{intra} .

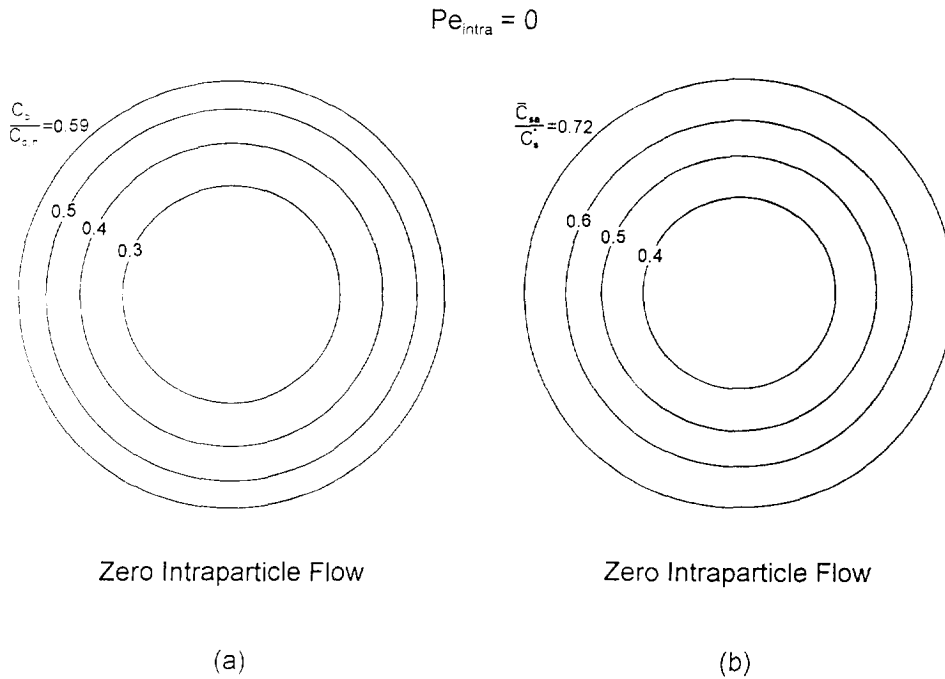


Fig. 4. Isoconcentration contours of the concentration of the adsorbate in the pore fluid of the macroporous region and in the adsorbed phase of the porous adsorbent particle when $d_m = 7.0 \cdot 10^{-7}$ m and $Pe_{intra} = 0$, at $x = 0.25 L$ and $t = 36$ min. (a) $C_p/C_{d,in}$; (b) \bar{C}_{sa}/C_s^* .

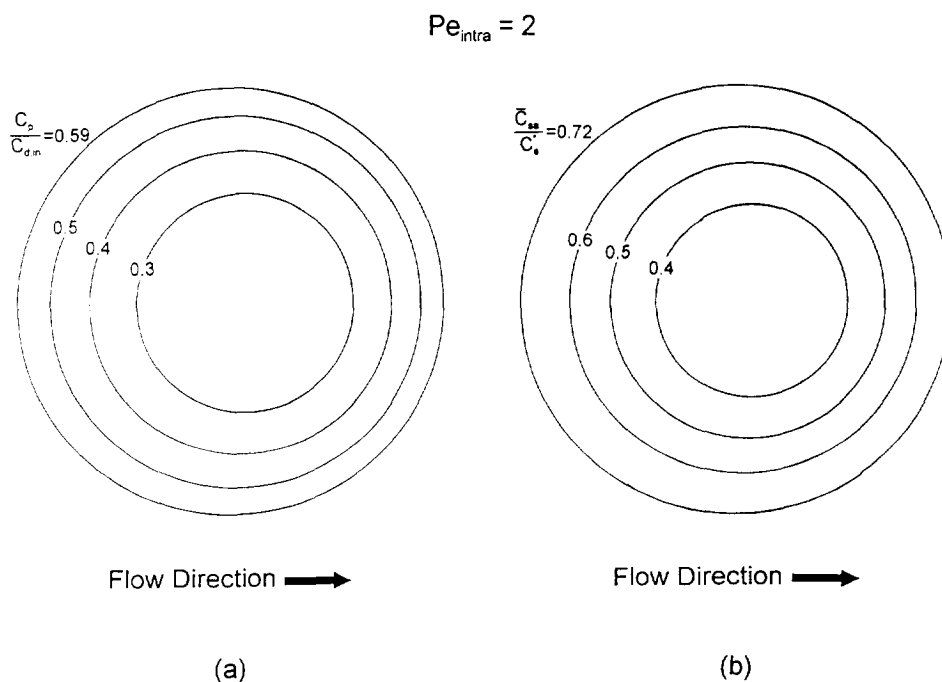


Fig. 5. Isoconcentration contours of the concentration of the adsorbate in the pore fluid of the macroporous region and in the adsorbed phase of the porous adsorbent particle when $d_m = 7.0 \cdot 10^{-7}$ m and $Pe_{intra} = 2$, at $x = 0.25 L$ and $t = 36$ min. (a) $C_p/C_{d,m}$; (b) \bar{C}_{sa}/C_s^* .

is a departure from spherical symmetry of the concentration profiles of the adsorbate as Pe_{intra} increases. As Pe_{intra} increases, the smallest concentration moves downstream and, thus, there is a higher adsorbate availability in the pore fluid of the macroporous region and a higher concentration of adsorbate in the adsorbed phase in the upstream half of the sphere than the downstream. This is due to the intraparticle fluid flow mechanism operating in the same direction as pore diffusion in the upstream part of the adsorbent particle but opposite to the pore diffusion mechanism downstream. Furthermore, the fluid moving by intraparticle convection to the downstream part of the adsorbent particle has limited adsorbate content since most of the adsorbate was already adsorbed upstream. The results in Figs. 4–7 also show that the magnitude of the departure from spherical symmetry of the concentration profiles of the adsorbate increases as the magnitude of the Pe_{intra} increases. Liapis et al. [5] have suggested that if the intraparticle

convective velocity could not be measured experimentally for a given kind of chromatographic porous adsorbent particles, then the behavior of the results in Figs. 4–7 could be considered to provide an indirect test for determining if a given kind of chromatographic adsorbent could exhibit perfusion behavior when the column is operated under conditions of interest to the user. If, for example, the concentration profiles of the adsorbate molecules in the adsorbed phase of the porous adsorbent particles could be determined experimentally, and if the experimentally determined concentration profiles show a departure from spherical symmetry, then this result could suggest that (considering that the adsorption sites on the surface of the pores were distributed evenly throughout the interior of the adsorbent particles) the porous adsorbent particles of the column may have exhibited perfusion behavior under the conditions of operation of the column. It should also be mentioned that model simulations using the values of the parameters in Table

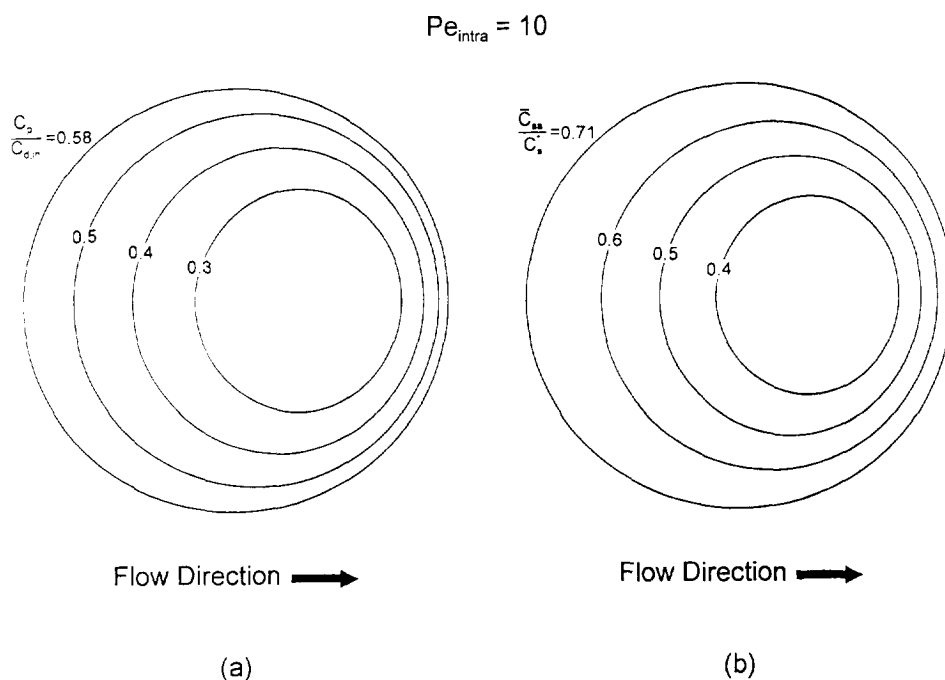


Fig. 6. Isoconcentration contours of the concentration of the adsorbate in the pore fluid of the macroporous region and in the adsorbed phase of the porous adsorbent particle when $d_m = 7.0 \cdot 10^{-7}$ m and $Pe_{\text{intra}} = 10$, at $x = 0.25 L$ and $t = 36$ min. (a) $C_p/C_{d,\text{in}}$; (b) \bar{C}_{sa}/C_s^* .

1, the values of the intraparticle Peclet numbers reported in Figs. 4–7, and considering the size of the microspheres to be either $d_m = 7.0 \cdot 10^{-8}$ m or $d_m = 7.0 \cdot 10^{-6}$ m, provided isoconcentration profiles whose behavior was similar to the behavior of the isoconcentration profiles presented in Figs. 4–7, as the value of Pe_{intra} was being increased.

In Fig. 8a, the dimensionless concentration profile of the adsorbate in the pore fluid of the pores of the macroporous region along the x_1 -axis ($x_1 = R \cos \theta$) is presented, while in Fig. 8b the dimensionless concentration profile of the adsorbate in the adsorbed phase of the adsorbent particle along the x_1 -axis is shown. In Fig. 8, results are presented for two different microsphere sizes and three different intraparticle Peclet numbers at position $x = 0.25L = 0.025$ m of the single fixed bed and at time $t = 36$ min. The results for the system with $d_m = 7.0 \cdot 10^{-8}$ m are not shown in Fig. 8; however, for the same value of Pe_{intra} the results obtained from the

system having $d_m = 7.0 \cdot 10^{-7}$ m were found to be almost identical to the results obtained from the system having $d_m = 7.0 \cdot 10^{-7}$ m. In Fig. 8, it can be observed that when $Pe_{\text{intra}} = 0$ (purely diffusive adsorbent particle) the concentration profiles are symmetrical, as expected, and the point of symmetry (concentration minimum) is located at the center of the particle where $x_1/R_p = 0$. When $Pe_{\text{intra}} > 0$ (perfusive adsorbent particle) the concentration profiles are not symmetrical and as Pe_{intra} increases the adsorbate concentration minimum moves downstream ($0 < (x_1/R_p) < 1.0$) while the overall adsorbate content of the spherical adsorbent particle increases. Furthermore, while the microsphere size, d_m , affects the values of C_p , \bar{C}_{sa} , and the values of the concentration minima, the results in Fig. 8 appear to indicate that the location of the concentration minima along the x_1 -axis of perfusive adsorbent particles ($Pe_{\text{intra}} > 0$) depends only on the value of the non-zero intraparticle Peclet number.

In Figs. 9 and 10, the dimensionless concen-

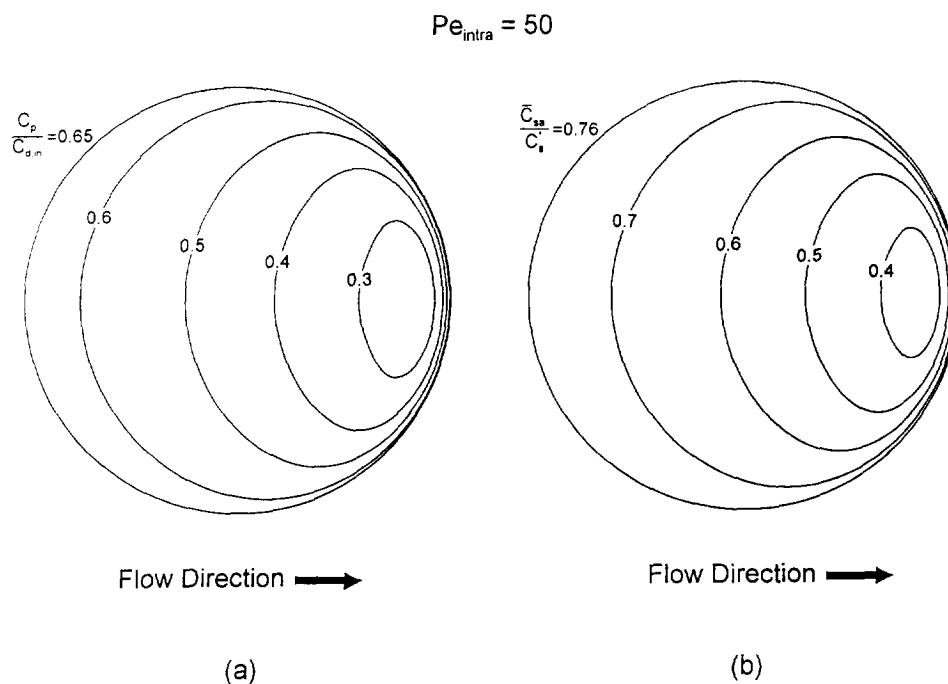


Fig. 7. Isoconcentration contours of the concentration of the adsorbate in the pore fluid of the macroporous region and in the adsorbed phase of the porous adsorbent particle when $d_m = 7.0 \cdot 10^{-7}$ m and $Pe_{\text{intra}} = 50$, at $x = 0.25 L$ and $t = 36$ min. (a) $C_p/C_{d,\text{in}}$; (b) \bar{C}_{sa}/C_s^* .

tration profiles of the adsorbate in the flowing stream and in the adsorbed phase are presented, respectively, for two different microsphere sizes and three different intraparticle Peclet numbers; the data in Figs. 9 and 10 have been obtained from the single fixed bed ($L = 0.1$ m) at time t when 1% breakthrough of the adsorbate [$C_d(t, L) = 0.01C_{d,\text{in}}$] occurs. The results for the system with $d_m = 7.0 \cdot 10^{-8}$ m are not shown in Figs. 9 and 10; however, for the same value of Pe_{intra} the results obtained from the system having $d_m = 7.0 \cdot 10^{-8}$ m were found to be almost identical to the results obtained from the system having $d_m = 7.0 \cdot 10^{-7}$ m. The results in Figs. 9 and 10 indicate that for the systems with $d_m = 7.0 \cdot 10^{-7}$ m the values of $C_d/C_{d,\text{in}}$ and \bar{C}_{sa}/C_s^* are equal to 1 for at least to $x = 0.05$ m, and this is the case when purely diffusive ($Pe_{\text{intra}} = 0$) or perfusive ($Pe_{\text{intra}} > 0$) adsorbent particles are used; of course it can be observed that the length x for which bed saturation has occurred is increased as the value of Pe_{intra} is increased. This

result indicates that it would be interesting to investigate the performance of the system with respect to the utilization of the adsorptive capacity of the particles in the bed, by dividing the column of length $L = 0.1$ m into two columns each of length $L/2 = 0.05$ m and operating these two columns in a periodic countercurrent mode. For the systems with $d_m = 7.0 \cdot 10^{-6}$ m, the values of $C_d/C_{d,\text{in}}$ and \bar{C}_{sa}/C_s^* are equal to 1 for at least to $x = 0.05$ m when perfusive adsorbent particles having $Pe_{\text{intra}} = 50$ are employed, while for the cases where $Pe_{\text{intra}} = 0$ and $Pe_{\text{intra}} = 10$ the results indicate that the values of $C_d/C_{d,\text{in}}$ and \bar{C}_{sa}/C_s^* are equal to 1 at least to about $x = 0.035$ m; of course, it can be observed again that the length x for which bed saturation has occurred is increased as the value of Pe_{intra} is increased. The results in Figs. 9 and 10 for the systems with $d_m = 7.0 \cdot 10^{-6}$ m indicate that it would be interesting to investigate the performance of the system with respect to the utilization of the adsorptive capacity of the particles in the

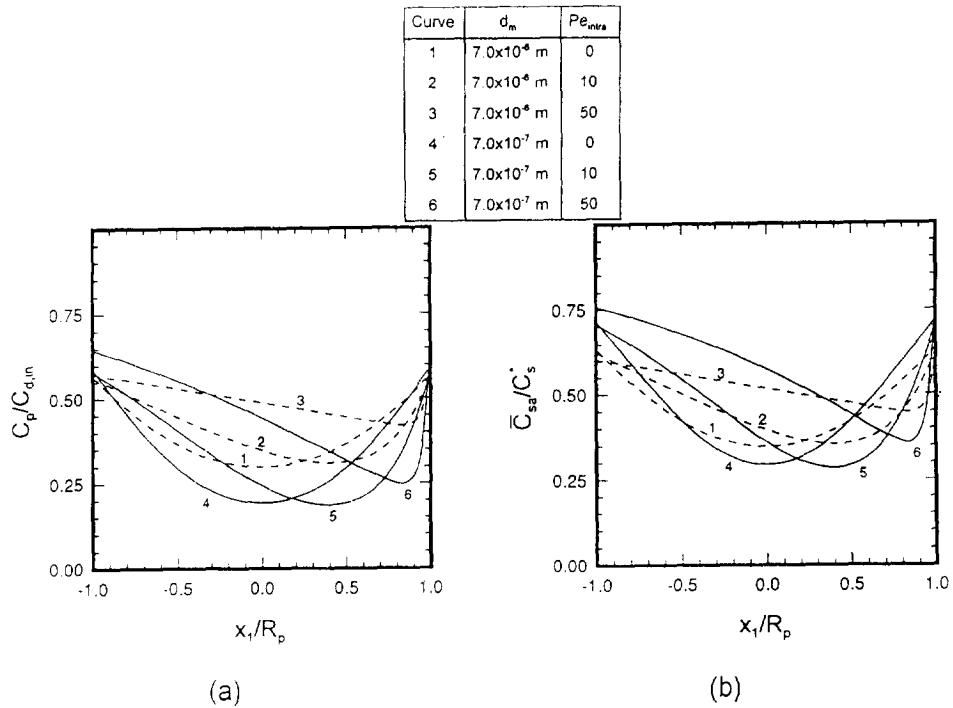


Fig. 8. Concentration profiles of the adsorbate in the pore fluid of the macroporous region and in the adsorbed phase of the porous adsorbent particle along the x_1 -axis of the particle for different values of the microsphere diameter, d_m , and intraparticle Peclet number, Pe_{intra} , at $x = 0.25 L$ and $t = 36$ min. (a) $C_p/C_{d,in}$; (b) C_{ad}/C_s^* .

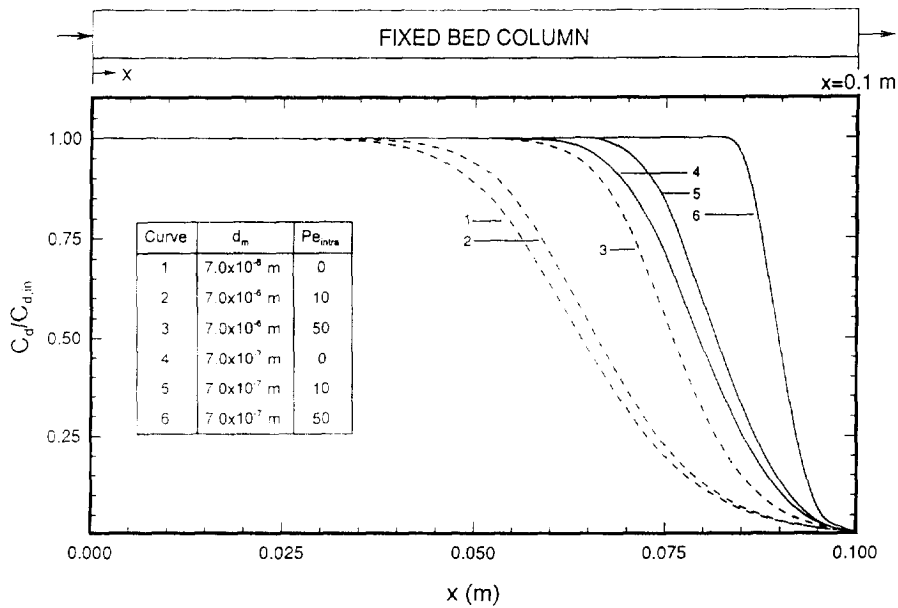


Fig. 9. Concentration profile of the adsorbate in the flowing fluid stream along the x -axis obtained from the single-column fixed-bed system at 1% breakthrough for different values of d_m and Pe_{intra} .

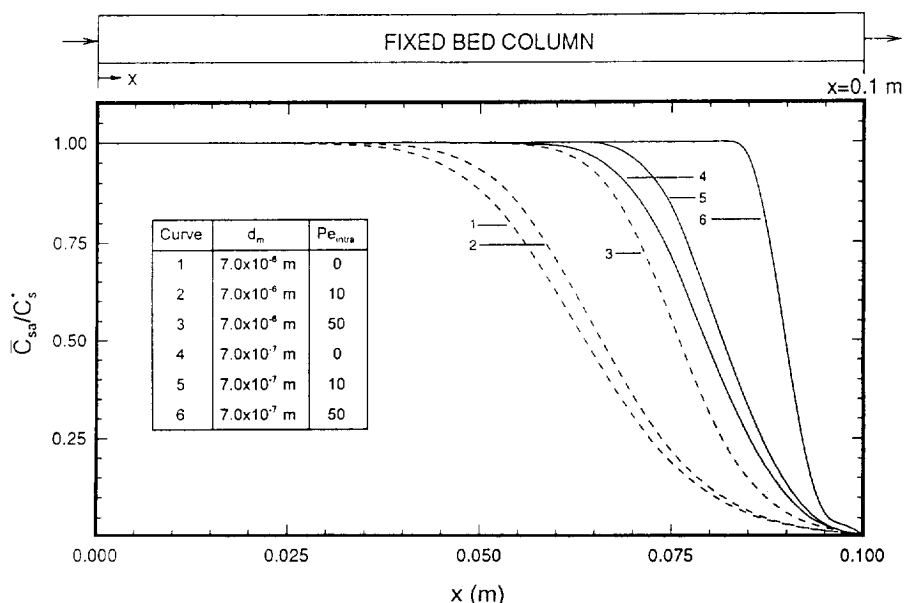


Fig. 10. Concentration profile of the adsorbate in the adsorbed phase along the x -axis obtained from the single-column fixed-bed system at 1% breakthrough for different values of d_m and Pe_{intra} .

bed, by dividing the column of length $L = 0.1$ m into three columns each of length $L/3 = 0.0333$ m and operating these three columns in a periodic countercurrent mode. It should be mentioned at this point that in this work the periodic countercurrent mode of operation has been studied only for the case where the column of length $L = 0.1$ m is divided into two columns each of length $L/2 = 0.05$ m, and then these two columns are operated in a periodic countercurrent mode.

When several beds are to be used in periodic countercurrent operation, then the criterion must be established for when to remove the spent bed at the upstream fluid end and to introduce a fresh bed at the other end. In this work, the criterion is to switch as soon as the exit concentration is equal to 1% of the inlet concentration [$C_d(t, L) = 0.01C_{d,in}$]; this implies that for the system studied in this work bed switching occurs at 1% breakthrough. Thus, in the two-column system under periodic countercurrent operation examined in this work, when the concentration in the effluent fluid reaches the limit of acceptability [$C_d(t, L) = 0.01C_{d,in}$], col-

umn switching takes place. The upstream column which is the more highly saturated is removed. The downstream column is moved up or switched to take its place, and a column of freshly regenerated anion-exchange adsorbent particles is added to become the new downstream column. After the first switch, the new upstream column will already be partly saturated, and therefore, the time to the second switch will be less than the time from start-up to the first switch, since in the latter case both columns initially contained fresh anion-exchange adsorbent particles. In the single-column system (Figs. 3–10) the whole bed of the anion-exchange adsorbent particles was also replaced when the exit fluid concentration was equal to 1% of the inlet concentration [$C_d(t, L) = 0.01C_{d,in}$].

In Figs. 11 and 12, the dimensionless concentration profiles of the adsorbate in the flowing fluid stream and in the adsorbed phase are presented, respectively, for two different microsphere sizes and three different intraparticle Peclet numbers, for the two-column system under periodic countercurrent operation. The

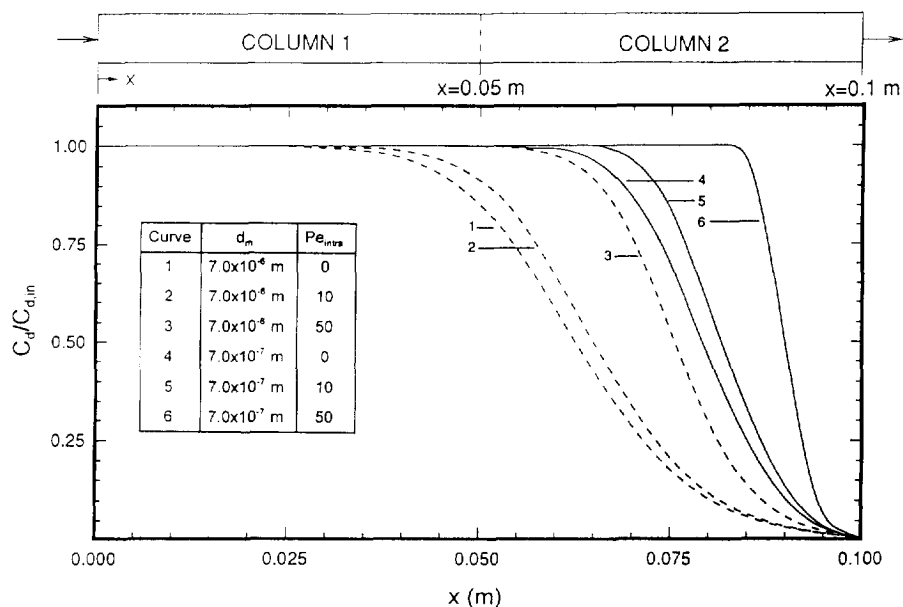


Fig. 11. Stabilized concentration profile at switching times of the adsorbate in the flowing fluid stream along the x -axis, obtained from the two-column periodic countercurrent system at 1% breakthrough for different values of d_m and Pe_{intra} .

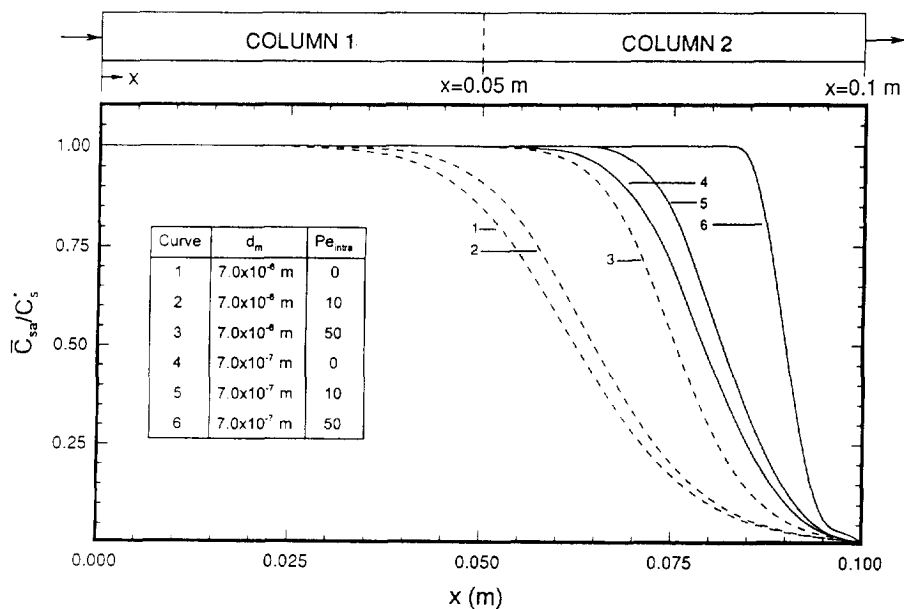


Fig. 12. Stabilized concentration profile at switching times of the adsorbate in the adsorbed phase along the x -axis, obtained from the two-column periodic countercurrent system at 1% breakthrough for different values of d_m and Pe_{intra} .

Table 2
Switching times for BSA adsorption into spherical bidisperse anion-exchange porous adsorbent particles when $d_m = 7.0 \cdot 10^{-8}$ m

Switch No.	Time elapsed between column switches for systems with different values of Pe_{intra} (min)								
	0 ^a	1	2	5	10	20	30	50	100
1	109	109	109	110	112	115	119	123	128
2	68	68	68	68	68	68	68	68	68
3	68	68	68	68	68	68	68	68	68
4	68	68	68		68				
5	68								

^a Pe_{intra} .

profiles in Figs. 11 and 12 are those obtained just prior to the second and subsequent switches. The results for the system with $d_m = 7.0 \cdot 10^{-8}$ m are not shown in Figs. 11 and 12; however, for the same value of Pe_{intra} the results obtained from the system having $d_m = 7.0 \cdot 10^{-8}$ m were found to be almost identical to the results obtained from the system having $d_m = 7.0 \cdot 10^{-7}$ m. A comparison of the results in Figs. 9 and 11 and in Figs. 10 and 12 indicates that the concentration profiles just prior to the first switch (Figs. 9 and 10), which also correspond to single-column operation, are essentially identical to the concentration profiles found just prior to the second and subsequent switches (Figs. 11 and 12). Thus, for a given set of values of d_m and Pe_{intra} one would expect that the time interval between successive switches after the first to be constant. The results in Tables 2, 3, and 4 confirm that this is the case. The time to the first switch would, of course, be equal to the period of the operating

cycle of the single-column system (Figs. 3–10). At this point, it is important to define the concept of the percentage utilization of the adsorptive capacity of a fixed bed. The total adsorptive capacity of a fixed bed is defined as the total amount of adsorbate in the adsorbed phase (in the column) at equilibrium (evaluated with respect to the value of $C_{d,in}$). The utilization of the adsorptive capacity of a fixed bed is defined as the ratio of the total amount of adsorbate in the adsorbed phase of the column when the desired breakthrough occurs (for example, 1% breakthrough) to the total adsorptive capacity of the column. The percentage utilization is obtained by multiplying the utilization of the adsorptive capacity of the column defined above by 100.

For the two-column system, the percentage utilization of the adsorptive capacity of the column removed is 100% when $d_m = 7.0 \cdot 10^{-8}$ m or $d_m = 7.0 \cdot 10^{-7}$ m for all values of the in-

Table 3
Switching times for BSA adsorption into spherical bidisperse anion-exchange porous adsorbent particles when $d_m = 7.0 \cdot 10^{-7}$ m

Switch No.	Time elapsed between column switches for systems with different values of Pe_{intra} (min)								
	0 ^a	1	2	5	10	20	30	50	100
1	109	109	109	110	112	115	119	123	128
2	68	68	68	68	68	68	68	68	68
3	68	68	68	68	68	68	68	68	68
4	68				68				
5	68								

^a Pe_{intra} .

Table 4

Switching times for BSA adsorption into spherical bidisperse anion-exchange porous adsorbent particles when $d_m = 7.0 \cdot 10^{-6}$ m

Switch No.	Time elapsed between column switches for systems with different values of Pe_{intra} (min)								
	0 ^a	1	2	5	10	20	30	50	100
1	88	88	88	89	91	96	100	104	110
2	66	66	66	66	67	68	68	68	68
3	67	67	67	67	68	68	68	68	68
4	67	67	67	67	67	68	68	68	68
5	67	67	67	67	67	68	68	68	68

^a Pe_{intra} .

traparticle Peclet number examined in this work ($0 \leq Pe_{intra} \leq 100$); when d_m is equal to $7.0 \cdot 10^{-6}$ m, the percentage utilization of the adsorptive capacity of the column removed is (a) 98.1% when $0 \leq Pe_{intra} \leq 2$, (b) 98.4% when $Pe_{intra} = 5$, (c) 99.2% when $Pe_{intra} = 10$, and (d) 100% when $20 \leq Pe_{intra} \leq 100$. For the single-column system, the percentage utilization of the adsorptive capacity of the column at 1% breakthrough (the

column is removed at 1% breakthrough), depends on the values of d_m and Pe_{intra} , and, for the systems studied in this work, it varies between 64.4% to 93.9%, as shown by the data of curves 1 and 2 of Fig. 13.

In Fig. 13, the relationship between the percentage utilization of the adsorptive capacity of the bed and the intraparticle Peclet number, Pe_{intra} , for the fixed-bed system (single-column)

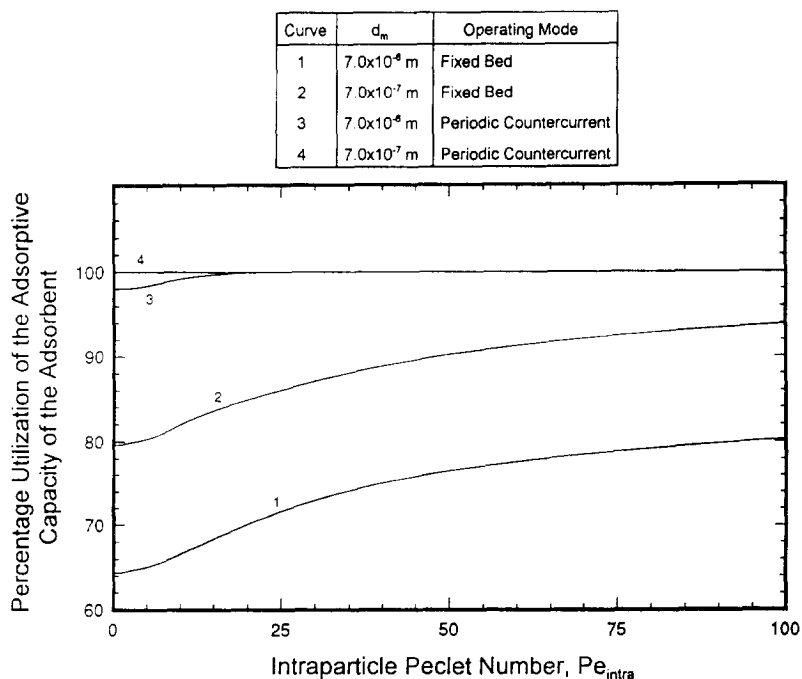


Fig. 13. Percentage utilization of the adsorptive capacity of the adsorbent versus intraparticle Peclet number, Pe_{intra} , obtained from single-column fixed-bed and two-column periodic countercurrent systems for different values of the microsphere diameter, d_m .

and the two-column system under periodic countercurrent operation is shown for two different values of d_m . The results for the systems with $d_m = 7.0 \cdot 10^{-8}$ m are not shown in Fig. 13, because the results for the systems having $d_m = 7.0 \cdot 10^{-8}$ m are almost identical to those obtained from the systems with $d_m = 7.0 \cdot 10^{-7}$ m. Curves 1 and 2 in Fig. 13 clearly show that for the single-column system the percentage utilization of the adsorptive capacity of the column depends on the values of d_m and Pe_{intra} , and the percentage utilization is increased as the value of d_m is decreased and the value of Pe_{intra} is increased. For the two-column system under periodic countercurrent operation, the results on curve 3 and line 4 indicate that this mode of operation provides higher values for the percentage utilization of the adsorptive capacity than all the values of the percentage utilization of the adsorptive capacity obtained from the single-column system for all values of d_m and Pe_{intra} used in this work. It is indeed a very interesting result when purely diffusive, $Pe_{intra} = 0$, adsorbent particles with $d_m = 7.0 \cdot 10^{-6}$ m are employed in a two-column system under periodic countercurrent operation, the percentage utilization of the adsorptive capacity obtained from such a system is higher than the percentage utilization obtained from a single-column system that uses perfusive adsorbent particles with $d_m = 7.0 \cdot 10^{-7}$ m and whose intraparticle Peclet number is equal to 100 ($Pe_{intra} = 100$). Also, the results in Tables 2, 3, and 4 indicate that in the two-column system the times between successive switches for all three different values of d_m and all nine different values of Pe_{intra} examined in this work are almost the same. This is because the adsorptive capacity of the column removed is almost completely saturated for all values of d_m and Pe_{intra} considered. Furthermore, when purely diffusive, $Pe_{intra} = 0$, or perfusive, $0 < Pe_{intra} \leq 100$, adsorbent particles with $d_m = 7.0 \cdot 10^{-8}$ m, or $d_m = 7.0 \cdot 10^{-7}$ m, or $d_m = 7.0 \cdot 10^{-6}$ m are employed in the two-column system under periodic countercurrent operation, all the anion-exchange adsorbent is removed about every 136 min (68 min + 68 min = 136 min), compared with every 128 min for the most efficient single-column

system which utilizes perfusive adsorbent particles with $d_m = 7.0 \cdot 10^{-8}$ m and $Pe_{intra} = 100$. Finally, from the data in Figs. 11–13 and in Tables 2, 3, and 4, the following very interesting result can be observed for the systems studied in this work: the factors of economic significance in the two-column system under periodic countercurrent operation, namely, the time between column switches and the degree of saturation of the column removed, are nearly independent of the values of the microsphere diameter, d_m , and of the intraparticle Peclet number, Pe_{intra} .

6. Conclusions and remarks

In this work, simulation studies involving the single-component adsorption of BSA into spherical anion-exchange porous adsorbent particles in a single-column fixed-bed system and in a two-column periodic countercurrent system in which the adsorbent is equally distributed over two beds (as shown in Fig. 1) were presented. The performance of chromatographic columns, as measured by the percentage utilization of the capacity of the adsorbent in the column and the time between bed switches for periodic countercurrent systems or the period of the operating cycle for single-column fixed-bed systems, was compared for both single-column fixed-bed and two-column periodic countercurrent systems for different values of the microsphere diameter, d_m , and the intraparticle Peclet number, Pe_{intra} . The total length of the two-column periodic countercurrent system was equal to the length of the single-column fixed-bed system.

The results for the single-column system indicate that as the microsphere size decreases and the intraparticle Peclet number increases the breakthrough curve becomes steeper and the time at which breakthrough starts is increased. Thus, the utilization of the capacity of the adsorbent particles of the single-column system is increased as d_m is decreased and Pe_{intra} is increased. However, Pe_{intra} must be greater than 10 for the percentage utilization of the adsorptive capacity of a single-column fixed-bed system

with perfusive particles to be significantly better than the percentage utilization of the adsorptive capacity of a single-column fixed-bed system with purely diffusive particles, as can be observed from the data of curves 1 and 2 of Fig. 13. Further, while the microsphere size affects the values of C_p , \bar{C}_{sa} , and the values of the concentration minima, the results of this work appear to indicate that the location of the concentration minima along the x_1 -axis of the adsorbent particle depends only on the value of the intraparticle Peclet number.

In the two-column periodic countercurrent system studied in this work, the concentration profiles of the adsorbate in the flowing fluid stream and in the adsorbed phase stabilize by the end of the first switch. The results show that in the two-column system, the times between successive switches for all three different values of d_m and all nine different values of Pe_{intra} examined in this work are almost the same. This is because the adsorptive capacity of the column removed is almost completely saturated for all values of d_m and Pe_{intra} considered. For the two-column system under periodic countercurrent operation, the results indicate that this mode of operation provides higher values for the percentage utilization of the adsorptive capacity than all the values of the percentage utilization of the adsorptive capacity obtained from the single-column fixed-bed system for all values of d_m and Pe_{intra} used in this work. In fact, the percentage utilization of the adsorptive capacity obtained from a two-column periodic countercurrent system having purely diffusive ($Pe_{intra} = 0$) adsorbent particles with the largest microsphere size studied in this work was found to be higher than the percentage utilization obtained from a single-column system that uses perfusive adsorbent particles with the smallest microsphere size and the largest intraparticle Peclet number studied in this work. Also, the results for the systems studied in this work suggest that there is no advantage in using perfusive particles instead of purely diffusive particles in the periodic countercurrent mode of operation when $d_m = 7.0 \cdot 10^{-8}$ m or $d_m = 7.0 \cdot 10^{-7}$ m, and only a very small advantage when $d_m = 7.0 \cdot 10^{-6}$ m.

Further, the following very interesting result was obtained from the simulation studies of the single-component adsorption system studied in this work: the factors of economic significance in the two-column system under periodic countercurrent operation, namely, the time between column switches and the degree of saturation of the column removed, are nearly independent of the values of the microsphere diameter, d_m , and of the intraparticle Peclet number, Pe_{intra} .

Acknowledgement

The authors gratefully acknowledge partial support of this work by Monsanto.

Symbols

A	Molecule of adsorbate
AS	Adsorbate–active site complex
C_d	Concentration of adsorbate in the flowing fluid stream of the column (kg/m^3 of bulk fluid)
$C_{d,m}$	Concentration of adsorbate at $x < 0$ when $D_L \neq 0$, or at $x = 0$ when $D_L = 0$ (kg/m^3 of bulk fluid)
\hat{C}_p	Concentration of adsorbate in the fluid of the macropores (through-pores) (kg/m^3 of macropore volume)
C_{pm}	Concentration of adsorbate in the fluid of the micropores (kg/m^3 of micropore volume)
\bar{C}_{ps}	Average concentration of adsorbate (kg/m^3 of perfusive particle)
C_s^*	Equilibrium concentration of adsorbate in the adsorbed phase given by Eq. 30, (kg/m^3 of perfusive particle)
\bar{C}_s	Average concentration of adsorbate (kg/m^3 of microparticle)
\bar{C}_{sa}	Average concentration of adsorbate in the adsorbed phase de-

	finned in Eq. 29 (kg/m^3 of perfusive particle)	R_p	Radius of perfusive particle (m)
C_{sm}	Concentration of adsorbate in the adsorbed phase of the microparticle (kg/m^3 of perfusive particle)	S	Active site
C_T	Maximum equilibrium concentration of adsorbate in the adsorbed phase of the microparticle (kg/m^3 of perfusive particle)	T	Temperature (K)
d_p	Diameter of spherical porous adsorbent particle ($d_p = 2R_p$) (m)	t	Time (s)
D_L	Axial dispersion coefficient of adsorbate (m^2/s)	v_p	Intraparticle velocity vector (m/s)
d_m	diameter of spherical microparticle ($d_m = 2r_m$) (m)	v_{pR}	Intraparticle velocity component along the R direction (m/s)
D_p	Effective pore diffusion coefficient of adsorbate in the macropores (through-pores) (m^2/s)	$v_{p\theta}$	Intraparticle velocity component along the θ direction (m/s)
D_{pm}	Effective pore diffusion coefficient of adsorbate in the micropores (m^2/s)	v_{px_1}	Axial component of the intraparticle velocity given by Eq. 9 (m/s)
$f(C_{pm}, C_{sm}, \mathbf{k})$	Functional form defined after Eq. 21	V_f	Column fluid superficial velocity (m/s)
F	Parameter given by Eq. 10 of Ref. [5]	x	Axial distance in column (m)
H	Parameter given by Eq. 11 of Ref. [5]	x_1, x_2, x_3	Space coordinates of perfusive particle as shown in Fig. 2 (m)
\mathbf{k}	Vector of adsorption rate constants defined after Eq. 21		
k_1	Adsorption rate constant in $A + S \xrightleftharpoons[k_2]{k_1} AS$ (m^3 of micropore volume/kg s)		
k_2	Adsorption rate constant in $A + S \xrightleftharpoons[k_2]{k_1} AS$ (s^{-1})		
K	Equilibrium adsorption constant of adsorbate, $K = k_1/k_2$ (m^3/kg)		
K_p	Particle permeability (m^2)		
L	Column length (m)		
Pe_{intra}	Intraparticle Peclet number [$Pe_{intra} = (v_{px_1} d_p)/D_p$]		
r	Radial distance in microparticle (m)		
r_m	radius of microparticle (m)		
R	Radial distance in perfusive particle (m)		

Greek letters

ε	Void fraction in column
ε_p	Macropore (through-pore) void fraction
ε_{pm}	Micropore void fraction
θ	Polar coordinate angle (radians)
ξ	Variable defined by Eq. (9) of Ref. [5]

References

- [1] A.I. Liapis and M.A. McCoy, J. Chromatogr., 599 (1992) 87.
- [2] M.A. McCoy, A.I. Liapis and K.K. Unger, J. Chromatogr., 644 (1993) 1.
- [3] A.I. Liapis, Math. Model. Sci. Comput., 1 (1993) 397.
- [4] A.I. Liapis and M.A. McCoy, J. Chromatogr. A, 660 (1994) 85.
- [5] A.I. Liapis, Y. Xu, O.K. Crosser and A. Tongta, J. Chromatogr. A, 702 (1995) 45.
- [6] A.I. Liapis and K.K. Unger, in G. Street (Editor), Highly Selective Separations in Biotechnology, Blackie Academic and Professional, An Imprint of Chapman and Hall, Glasgow, 1994, pp. 121–162.
- [7] N.B. Afeyan, N.F. Gordon, I. Mazsaroff, L. Varady, S.P. Fulton, Y.B. Yang and F.E. Regnier, J. Chromatogr., 519 (1990) 1.
- [8] N.B. Afeyan, S.P. Fulton, N.F. Gordon, I. Mazsaroff, L. Varady and F.E. Regnier, Biotechnology, 8 (1990) 203.
- [9] A.I. Liapis and D.W.T. Rippin, AIChE J., 25 (1979) 455.

- [10] B.H. Arve and A.I. Liapis, *Biotechnol. Bioeng.*, 32 (1988) 616.
- [11] F.H. Arnold, H.W. Blanch and C.R. Wilke, *Chem. Eng. J.*, 30 (1985) B25.
- [12] F.H. Arnold, H.W. Blanch and C.R. Wilke, *Chem. Eng. J.*, 30 (1985) B9.
- [13] G. Neale, N. Epstein and W. Nader, *Chem. Eng. Sci.*, 28 (1973) 1865.
- [14] Y. Xu, *Internal Report, Department of Chemical Engineering, University of Missouri-Rolla, MO, 1994.*